Rev.Adv.Mater.Sci. 25 (2010) 32-41

CHARACTERIZATION OF SEVERE PLASTIC DEFORMATION TECHNIQUES WITH RESPECT TO NON-MONOTONITY

K. Bobor and Gy Krallics

Department of Materials Science and Engineering, Budapest University of Technology and Economics, 1111 Budapest Bertalan Lajos u. 7., Hungary

Received: December 12, 2009

Abstract. The method of severe plastic deformation (SPD) is often used to produce bulk ultrafine grained materials. SPD is a procedure, whereby the structure of the material changes from the initial coarse grained state to ultra-fine grained structure. For these techniques shear deformation as well as the so-called non-monotonic deformation are characteristic. The aim of this paper is to compare different metal-forming techniques with respect to non-montonity of deformation. A quantity and its calculation for the characterization of non-monotonity are introduced. Study of different metal-forming processes (simple shear, ECAP, equal and differential speed rolling) concerning non-monotonity and the comparison of these results are presented.

1. INTRODUCTION

The method of severe plastic deformation (SPD) is often used to produce bulk ultra-fine grained materials (UFG). SPD is a procedure, whereby the structure of the material changes from the initial coarse grained state to ultra-fine grained structure. For the evolved microstructure is the ~70-500 nm average grain size characteristic. Numerous methods exist, which are able to produce a material with the above mentioned structure in a smaller or larger volume (Accumulative roll bonding [1,2], Equal channel angular extrusion [3,4], High pressure torsion [5], Repetitive corrugation and straightening [6]). Investigated the mechanical schema of the procedures, we searched for such attributes, which characterize the mentioned techniques, and at the same time a measure was searched for, with the methods can be distinguished from each other.

By our previous researches can be established, that for these techniques shear deformation as well as the so-called non-monotonic deformation are characteristic. This mechanical concept was introduced by Smirnov-Aljajev [7]. By definition, the process develops monotonically if no component of the rate of deformation tensor changes its sign, namely the eigenvectors of the rate of deformation tensor are parallel to the same material lines during the

Corresponding author: Gy Krallics, e-mail: krallics@eik.me.hu

whole deformation process and the Lode parameter remains constant. By a non-monotonic deformation the comparative state of the material lines and the eigenvectors of the rate of deformation tensor are changing during the process.

According to our assumption by equal amount of deformation by the forming process with stronger non-monotonity stronger grain refinement occurs, than by a process which is monotonic or close to the monotonic state. A microstructure with finer grains is expected by a less monotonic deformation. The under mentioned mechanical analysis was performed to investigate the problem of non-monotonity.

2. MONOTONITY OF FORMING PROCESSES

The mechanical concept of monotonity was introduced by Smirnov-Aljajev [7]. A forming process develops monotonically if no component of the rate of deformation tensor changes its sign, namely the eigenvectors of the rate of deformation tensor are parallel to the same material lines during the whole deformation process and the Lode parameter remains constant. The two necessary conditions for a monotonic deformation that the relative state of the material lines and the eigenvectors of the rate of deformation tensor are not changing during the process, and the Lode parameter remains constant. Investigating the monotonity of the forming processes, can be distinguished which are monotonic processes and which are further or closer to the monotonic state. The second condition bears a relation to the stress state, which has no direct relation to the evolving microstructure. To ascertain more about the microstructural processes, the study of the firs condition is necessary. Through the investigation of the type of the deformation, a measure can be created, which is appropriate to describe the degree of non-monotonity of a forming process.

In the interest of that different processes could be investigated and compare with respect to the monotonity, this characteristic measure is needed. The definition and calculation of the degree of non-monotonity (DNM) for some forming processes will be showed in the next chapters.

3. DEGREE OF NON-MONOTONITY

3.1. Definition

In this chapter the definition of a degree of non-monotonity (DNM) is shown, with the calculation in different coordinate systems. To define the monotonity, or rather the non-monotonity, the separate analysis of the rigid body rotation of a material particle and the rotation of the eigenvectors of the rate of deformation tensor **d** is necessary. Both values can be deduced from the velocity gradient tensor **L**, hence an appropriate description of the velocity field of the forming process is required. The starting point of the analysis that the velocity field is given in the function of the time *t* and the space *x* as following

$$\boldsymbol{v} = \begin{bmatrix} \mathrm{v}_1(\boldsymbol{x},\mathrm{t}) \\ \mathrm{v}_2(\boldsymbol{x},\mathrm{t}) \\ \mathrm{v}_3(\boldsymbol{x},\mathrm{t}) \end{bmatrix}. \tag{1}$$

From this, the velocity gradient tensor can be deduced through the covariant derivative.

$$L_{kl} = \mathrm{v}_{k;l} = \mathrm{v}_{k,l} + \mathrm{v}_s \Gamma^s_{kl}, \tag{2}$$

where Γ^s_{kl} is the second order Christoffel symbol. So the velocity gradients in Cartesian and cylindrical coordinate systems are the following:

$$L_{(x,y,z)} = \begin{bmatrix} \frac{\partial \mathrm{v}_1}{\partial x_1} & \frac{\partial \mathrm{v}_1}{\partial x_2} & \frac{\partial \mathrm{v}_1}{\partial x_3} \\ \frac{\partial \mathrm{v}_2}{\partial x_1} & \frac{\partial \mathrm{v}_2}{\partial x_2} & \frac{\partial \mathrm{v}_2}{\partial x_3} \\ \frac{\partial \mathrm{v}_3}{\partial x_1} & \frac{\partial \mathrm{v}_3}{\partial x_2} & \frac{\partial \mathrm{v}_3}{\partial x_3} \end{bmatrix}, \tag{3}$$

$$L_{(r,\phi,z)} = \begin{bmatrix} \frac{\partial \mathrm{v}_1}{\partial x_1} & \frac{1}{x_1}\frac{\partial \mathrm{v}_1}{\partial x_2} - \frac{v_2}{x_1} & \frac{\partial \mathrm{v}_1}{\partial x_3} \\ \frac{\partial \mathrm{v}_2}{\partial x_1} & \frac{1}{x_1}\frac{\partial \mathrm{v}_2}{\partial x_2} + \frac{v_1}{x_1} & \frac{\partial \mathrm{v}_2}{\partial x_3} \\ \frac{\partial \mathrm{v}_3}{\partial x_1} & \frac{1}{x_1}\frac{\partial \mathrm{v}_3}{\partial x_2} & \frac{\partial \mathrm{v}_3}{\partial x_3} \end{bmatrix}. \tag{4}$$

The rigid body rotation ω is described through the antisymmetric and the rate of deformation **d** through the symmetric part of **L** using the Eq. (5).

$$\mathbf{d}_{kl} = \frac{\mathbf{L}_{kl} + \mathbf{L}_{lk}}{2}, \quad \boldsymbol{\omega}_{kl} = \frac{\mathbf{L}_{kl} - \mathbf{L}_{lk}}{2}. \tag{5}$$

The ω tensor can be transcribed into vector form using Eq. (6).

$$\boldsymbol{\omega} = \begin{bmatrix} 0 & -\omega_3 & \omega_2 \\ \omega_3 & 0 & \omega_1 \\ -\omega_2 & -\omega_1 & 0 \end{bmatrix}, \qquad \boldsymbol{\omega} = \begin{bmatrix} \omega_1 \\ \omega_2 \\ \omega_3 \end{bmatrix}. \tag{6}$$

The ω vector gives the axis and the angular velocity of the rotation for a material point at the given coordinates at the given time. To study the non-monotonity also needed, how the eigenvectors of the rate of deformation tensor rotate through the forming process.

Let $\boldsymbol{n}_1$, $\boldsymbol{n}_2$, and $\boldsymbol{n}_3$ denotes the eigenvectors. To define the rotation of an eigenvector according to Fig. 1, Eqs. (7) and (8) can be used:

$$\dot{\boldsymbol{n}}_i = \boldsymbol{\Omega} \times \boldsymbol{n}_i , \tag{7}$$

$$\dot{\boldsymbol{n}}_i = \boldsymbol{\Omega} \cdot \boldsymbol{n}_i , \tag{8}$$

where Ω is the vector of the rotation. This can be expressed also as Ω antisymmetric tensor, similar to ω in Eq. (6). Since the Ω vector can be determined from the knowledge of at least three vectors, hence all eigenvectors must be known. By the calculation of $\dot{\boldsymbol{n}}_i$ the material derivative must be used according to Eq. (9), to obtain a quantity connected to the material.

$$\dot{\boldsymbol{n}} = \frac{\partial \boldsymbol{n}}{\partial t} + \boldsymbol{v}^k \boldsymbol{n}_{s;k} . \tag{9}$$

The $\dot{\boldsymbol{n}}_i$ and n_i vectors can be arranged into **N** and $\dot{\mathbf{N}}$ matrices, so the Eq. (10) can be created, and solved for **W** according to the Eq. (11).

$$\dot{\mathbf{N}} = \boldsymbol{\Omega} \cdot \mathbf{N} . \tag{10}$$

$$\dot{\mathbf{N}}\mathbf{N}^{1} = \boldsymbol{\Omega} . \tag{11}$$

One of the necessary conditions of monotonity, that the eigenvectors of the rate of deformation coincide with the same material line through the whole deformation. This condition is fulfilled if Ω and ω vectors are equal. If the difference between the vectors **b** = ω - Ω differ from 0 then the process is non-monotonic in the given time for the given material point. In order to characterize the deformation of a chosen material particle through the forming process, the integration of **b** over the time and along a particle trajectory is needed. There are two possibilities to calculate this integral according to Eqs. (12) and (13).

$$\mu_1 = \int_0^1 |\beta| \, dt, \tag{12}$$

$$\mu_1 = \left| \int_0^1 \beta \, dt \right| . \tag{13}$$

The both value of μ_1 and μ_2 are zero or positive. μ_1 is increasing or remains constant in time, while μ_2 can take more times the initially zero value. μ_1 is a cumulative measure which summarizes the effect non-monotonic type deformation. μ_2 is a relative measure which represents the relative state of the eigenvectors of **d** and the material lines compare to the initial state. If μ_2 equal zero then this relative state is the same as at t=0. The more the value of μ_2 the more rotation occurred compare to the initial state.

3.2. Definition for discontinuity surfaces

Analytical models are often used to modeling a forming process. In this paper analytical models were also used for the calculations. These contain mostly simplification in order of faster and easier calculus. They are not as accurate as a finite element computation, but provide a continuous velocity field.

By these methods discontinuity surfaces are often used to simplify the flow model. The velocity of a particle which is passing through this surface has a stepwise change (Fig. 2). The normal component to the surface A_f remains continuous ($\mathbf{n}_n^+=\mathbf{n}_n^-$) but the tangential changes are abrupt. The material particle is deformed infinitely rapid; hence the calculation of the DNM on these surfaces is not trivial.

The velocity vector can be decomposed to a $\mathbf{n}_n$ normal and a $\mathbf{n}_t$ tangential component immediately before and after the A_f surface. The normal components are equal on the both side of the discontinuity surface A_f ($\mathbf{n}_n^+=\mathbf{n}_n^-$), while the tangential components are changing from $\mathbf{n}_t^+$ to $\mathbf{n}_t^-$. Take two parallel surfaces before and after A_f. Make an assumption, that in the d wide small region between A_f^+ and A_f^- normal component $\mathbf{n}_n$ is constant, while the tangential component is changing linear from $\mathbf{n}_t^+$ to $\mathbf{n}_t^-$. The velocity gradient can be defined for this small region according to Eq. (14).

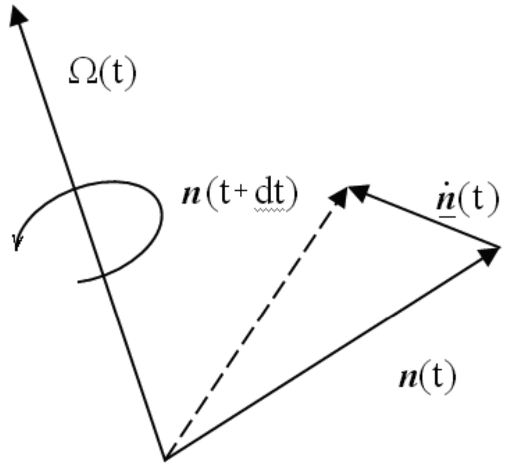

Fig. 1. Rotation of the eigenvector $\boldsymbol{n}_i$.

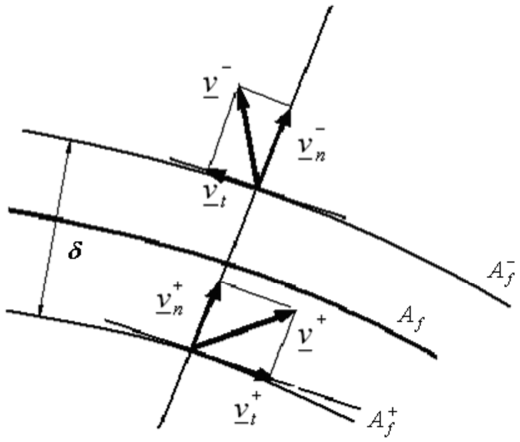

Fig. 2. Velocity components by a discontinuity field.

$$\mathbf{L} = \begin{bmatrix} 0 & 0 & 0 \\ \frac{\Delta v_t}{\delta} & 0 & 0 \\ 0 & 0 & 0 \end{bmatrix},$$

$$\mathbf{d} = \begin{bmatrix} 0 & \frac{\Delta v_t}{2\delta} & 0 \\ \frac{\Delta v_t}{2\delta} & 0 & 0 \\ 0 & 0 & 0 \end{bmatrix},$$

$$\boldsymbol{\omega} = \begin{bmatrix} 0 & -\frac{\Delta v_t}{2\delta} & 0 \\ \frac{\Delta v_t}{2\delta} & 0 & 0 \\ 0 & 0 & 0 \end{bmatrix}, \qquad (14)$$

where $\Delta \boldsymbol{v}_t = \boldsymbol{v}_t^- - \boldsymbol{v}_t^+$. In the δ wide region the eigenvectors of **d** are unchanged Ω=0, while a rigid body rotation occurs. If a material particle passing through this region in τ_0 time, then the $\delta = \mathbf{n}_n t_0$ relation is valid. Through the integration of the quantities the DNM and the equivalent strain can be expressed according to Eqs. (15) and (16).

$$\mu_{1,2} = \int_0^{t_0} \frac{\Delta v_t}{2\delta} dt = \int_0^{t_0} \frac{\Delta v_t}{2 v_n t_0} dt = \frac{\Delta v_t}{2 v_n t_0} \int_0^{t_0} dt = \frac{\Delta v_t}{2 v_n t_0} \frac{t_0}{t_0} = \frac{\Delta v_t}{2 v_n t_0}, \qquad (15)$$

$$\varphi = \frac{\Delta v_t}{\sqrt{3} v_n}. \qquad (16)$$

The relation between DNM and equivalent strain is described in the Eq. (17).

$$\varphi = \frac{\Delta v_t}{\sqrt{3} v_n}. \qquad (17)$$

4. CHARACTERISTIC DEFORMATION OF DIFFERENT FORMING PROCESSES

4.1. Simple shear

The velocity field for simple shear is given in a Cartesian coordinate system using Eq. (18) with a parameter *k*.

$$\boldsymbol{v}_{(x,y,z)} = \begin{bmatrix} k \cdot x_2 \\ 0 \\ 0 \end{bmatrix}. \qquad (18)$$

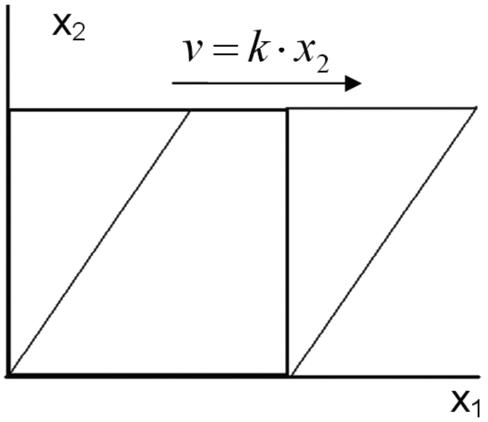

Fig. 3. Simple shear.

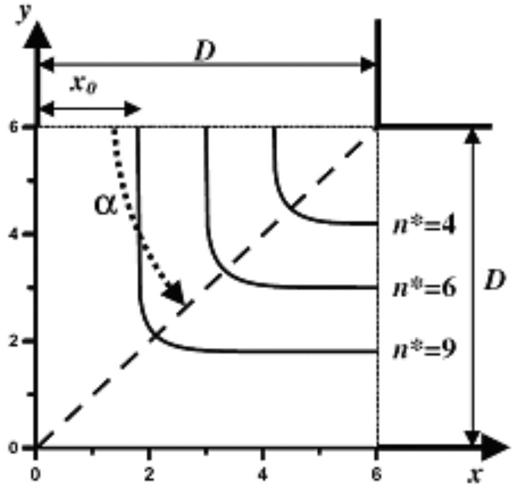

Fig. 4. Flowline model of ECAP, see [4] for more details.

Simple shear (Fig. 3) is the way of deformation - strongly non-monotonic – in the idealized process of ECAP and HPT. The DNM is increasing linear with increasing strain according to $\mu_{1,2} = \frac{\sqrt{3}}{2}\varphi$. In this case μ_1 and μ_2 are equal.

4.2. Uniaxial tension

By tension of a bar with a circular cross section the velocity field in a cylindrical coordinate system can be described using Eq. (19).

$$\boldsymbol{v}_{(r,\phi,z)} = \begin{bmatrix} \frac{x_1 v_0}{2h} \\ 0 \\ -\frac{x_3 v_0}{h} \end{bmatrix}, \quad (19)$$

where $h=h_0-v_0 t$ the actual height of the specimen. By uniaxial tension neither rigid body rotation nor rotation of eigenvectors of **d** occurs, so the DNM is zero. By the uniaxial tension μ_1 and μ_2 are equal.

4.3. ECAP

There are several analytical modes for ECAP, one of them was used [4], where the material points are moving through a trajectory described in Eq. (20) (Fig. 4), where x_0 is the initial coordinate, and n a parameter.

$$\boldsymbol{v}_{(x,y,z)} = \begin{bmatrix} v_0 \left(\frac{D - x_2}{D - x_0} \right)^{n-1} \\ -v_0 \left(\frac{D - x_1}{D - x_0} \right)^{n-1} \\ 0 \end{bmatrix}. \quad (20)$$

For the calculation of DNM a sample with D=6 mm was investigated by the point x_0=1.5, 3, 4.5 mm, with n=9, 6, 4. The deformations were calculated after more passes according to the routes A, B_A, B_C, and C [8]. The results are summarized in the chapter 5.

4.4. Equal and differential speed rolling

For equal (symmetric) and differential speed (asymmetric) rolling the analytical model of [9] was used (Fig. 5). This model describes the velocity field according to the Eqs. (21), (22), and (23). After F discontinuity surface, the material particles are flowing on a circular arc.

$$v_x = -\frac{v_0 H_0}{H_x}\left[1-\frac{2ax_2\left(1-\frac{\beta H_x}{H_0}\right)}{H_1}\right],$$

$$v_y = -v_0 H_0 \left[\frac{x_2\left(1-\frac{ax_2}{H_1^2}\right)}{H_x^2}-\frac{a\left(1-2\frac{\beta H_x}{H_0}\right)}{4H_1}\right]\frac{\partial H_x}{\partial x}. \qquad (21)$$

$$H_x = H_1 + 2R - 2\sqrt{\left(R^2 - x_1^2\right)},$$

$$H_1 + 2R - 2\sqrt{\left(R^2 - x_1^2\right)},$$

$$H_A = \sqrt{\left(\frac{\omega_2}{\omega_1}\right)}B,$$

$$H_c = \frac{H_A + H_B}{2}, \qquad (22)$$

$$H_B = \sqrt{\left(\frac{\omega_1}{\omega_2}\right)}B,$$

$$B = \sqrt{\left(H_0 H_1\right)}\left(\frac{H_1}{H_0}\right)^{\left(\frac{\alpha}{2\psi}\right)} e^{\left(-\frac{\alpha^2}{16\psi}\right)},$$

$$K = \frac{H_0^2 - H_1^2}{2H_1^2} + \frac{2\beta\left(H_0^3 - H_1^3\right)}{3H_1^2 H_0},$$

$$a = \frac{\alpha\psi\left(H_A - H_B\right)}{H_1 K}, \qquad (23)$$

$$\beta = \frac{\dfrac{2H_0\left(1+\frac{H_1}{H_0}+\frac{H_1^2}{H_0^2}\right)}{3H_1} - \left(1+\frac{H_1}{H_0}\right)}{\dfrac{H_0\left(1+\frac{H_1}{H_0}\right)\left(1+\left(\frac{H_1}{H_0}\right)^2\right)}{2H_c} - \dfrac{2\left(1+\frac{H_1}{H_0}+\left(\frac{H_1}{H_0}\right)^2\right)}{3}}.$$

where ν_0 is the velocity before the rolls, H_0 and H_1 are the initial and final thickness, ψ is the Kudo friction coefficient, and ω_1 and ω_2 the angular velocities of the rolls.

The deformation of a plate of 16 mm initial thickness was studied during the rolling to 11 mm and further to 7, 4, 2, 5, and, finally, to 1.5 mm. The rolls had a diameter of ∅140 mm. By the asymmetric rolling a speed ration of 1:2 and the route UD [10] was applied. By route UD both μ_1 and μ_2 are equal through the passes.

By equal speed rolling in the center of the plate the type of deformation is pure montonic tension, the DNM equal zero. Towards to the surface the DNM is increasing with the distance from the center. If the rolling speeds are not equal, then the deformation also in the center of the material becomes non-monotonic, a shear-like deformation component appears.

5. RESULTS AND DISCUSSION

The definition of DNM and their calculation for some forming processes was shown. The monotonity or rather the non-monotonity of these forming techniques was presented. In Fig. 6 the results of the DNM calculation are shown for the above presented forming processes. There can be observed, that the simple shear has a highest m_1 value, and the other processes located between simple shear and the monotonic uniaxial tension. It shows that the ECAP model – which describes the process more realistic – mentioned in the section 4.3 is quite close to the simple shear, to the idealized type of deformation of ECAP and HPT.

Fig. 7 shows that the μ_1 value is increasing with the deformation independent from the routes. Contrarily, Fig. 8 shows that the μ_2 value is different for every route. In cases of routes A and B_A it is increasing continuously, while by route B_C after every fourth and by route C after every second pass takes the initial zero value.

The difference between the conventional (ESR) and the different speed rolling (DSR) is also considerable. By the ESR in the middle of the plate the DNM is low, the deformation is mainly tension, and the shear is not dominant. Toward to the surface, the shear-like deformation becomes more dominant, the DNM is increasing, but lag behind the case of the different speed rolling. By the latter the DNM is relative high for the whole cross section, the shear deformation is dominant in the centre also. By uniaxial tension the value of the DNM remains zero according to the requirements.

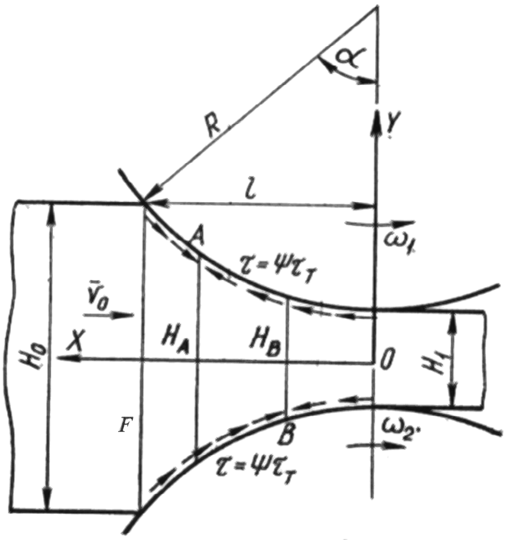

Fig. 5. Flowline model of plain rolling, data from [9].

Our initial assumption was that by equal amount of deformation by the forming process with stronger non-monotonity stronger grain refinement occurs. To verify this assumption, the evolved microstructures must be investigated.

Several authors made experiments and investigations about the grain refinement by the mentioned forming processes.

The grain refinement effect of ECAP process on various materials was investigated by several authors. Furukawa *et al*. have analysed the deformation paths of the different routes through the shape alteration of a cube [11]. This is in accordance with the values of μ_2, which characterize the actual and initial relative state of the material lines and eigenvectors of the rate of deformation. In cases of routes A and B_A the cube deforms continuously with the passes, while the cyclic repetition is characteristic for the routes B_C and C. In case of route C the shape returns to the initial after two passes, by the route B_C after four passes. The above mentioned results are in accordance with these, Fig. 8 shows the continuous increasing of μ_2 by the routes A and B_A and the cyclic repetition by routs B_C and C.

M. Kawasaki *et al*. have made experiments with pure aluminium [12,13], I. V. Aleksandrov *et al*. with copper [14], J. Gubicza *et al*. with AZ91 magnesium alloy [15]. These and other studies can be found in the literature supports that the ECAP is one of the most appropriate techniques to produces

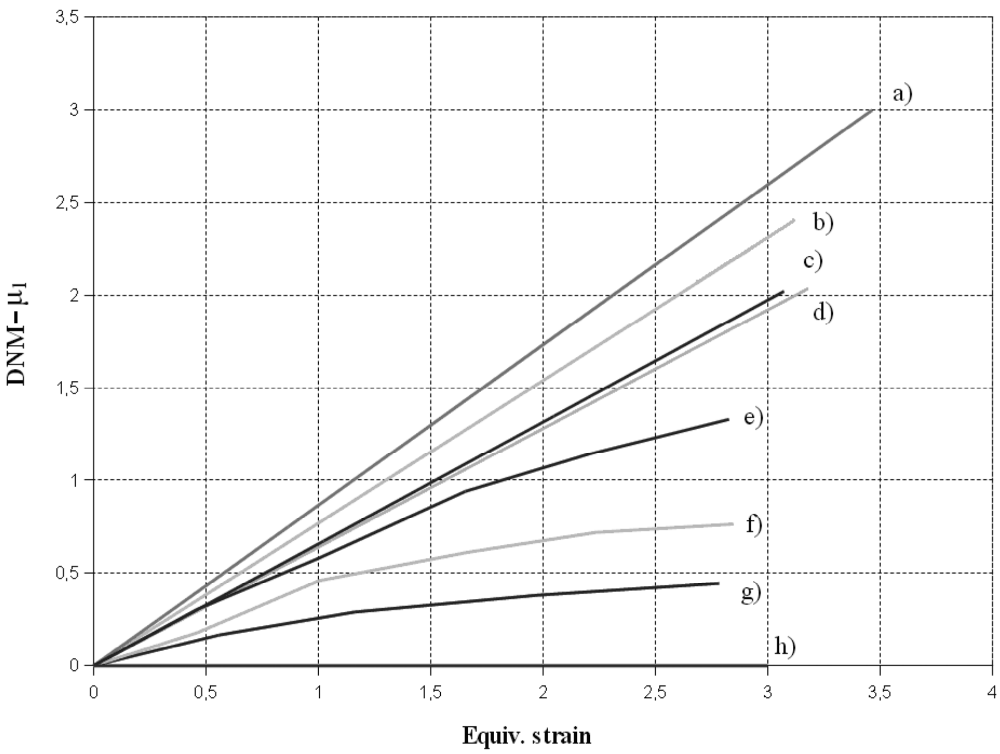

Fig. 6. Comparison of DNM (m_1) for forming processes. (a) Simple shear; (b) ECAP (*n*=4, x_0=1,5 mm, route A); (c) ECAP (*n*=6, x_0=3 mm, route A); (d) ECAP (*n*=7, x_0=4.5 mm, route A); (e) DSR surface; (f) DSR center; (g) ESR surface; (h) Tension, ESR center.

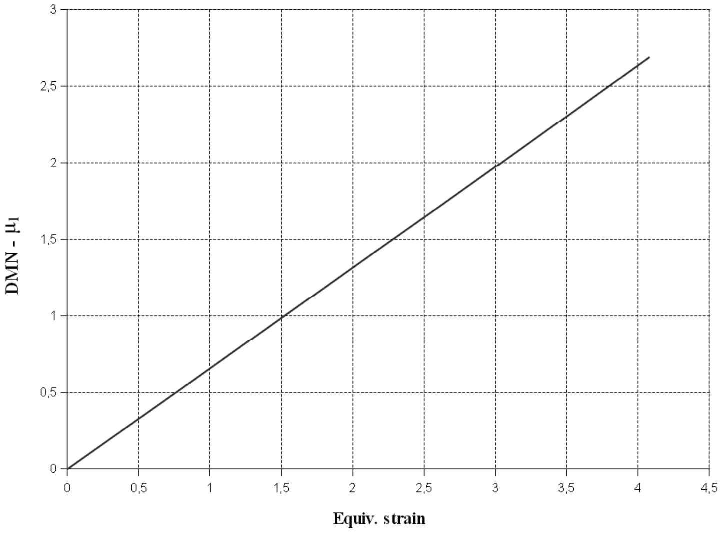

Fig. 7. The μ_1 DNM values for ECAP all routes (x_0=3 mm, n=6).

an UFG microstructure. The different deformation routes create different microstructures; the ratio of the low and high angle boundary, the shape of the grains and the texture are different. If the grain size is observed, it can be established that independent from the routes a microstructure with a similar average grain size is created [16-20]. The values of μ_1 are equal for all cases, which is in accord with our initial assumption, that by same DNM (μ_1) a similar degree of grain refinement can be expected.

Besides the ECAP, the grain refinement effect of HPT is similarly good [21,22]. Through ECAP or HPT a microstructure with the average grain size under 1 μm can be produced, and hereby these are ones of the most effective SPD processes. This corresponds with the recent calculations, where the

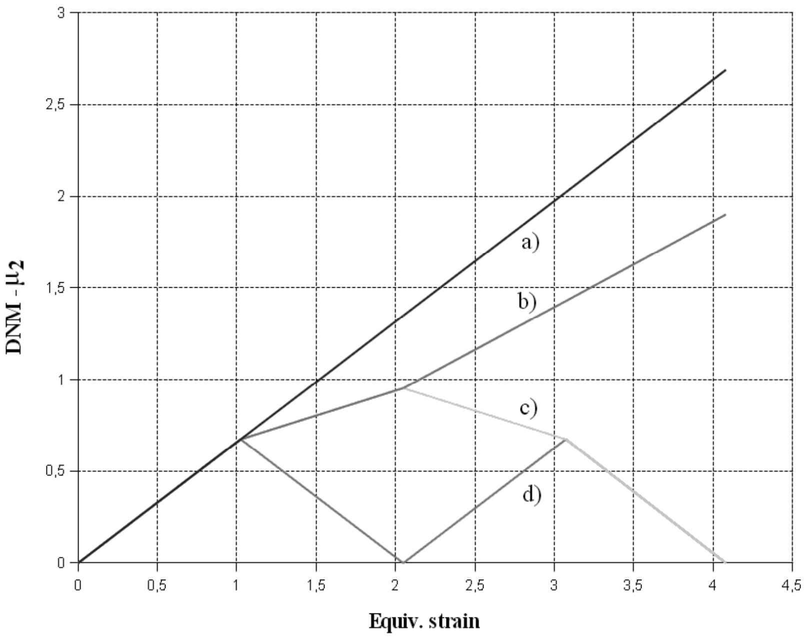

Fig. 8. The μ_2 DNM values for ECAP routes. (a) ECAP (n=6, x_0=3 mm, route A); (b) ECAP (n=6, x_0=3 mm, route B_A); (c) ECAP (n=6, x_0=3 mm, route B_C); (d) ECAP (n=6, x_0=3 mm, route C).

simple shear (idealised HPT and ECAP) and the ECAP have the highest degree of non-monotonity.

W.J. Kim *et al.* performed experiments with equal and differential speed rolling of copper [23]. Theirs results show that stronger grain refinement occurs through the differential speed rolling. W.J. Kim *et al*. performed DSR on AZ91 magnesium alloy, and investigated the evolved microstructure [24]. They compared the result with the microstructures produced by ECAP, accumulative roll bonding and extrusion. They showed that the grain refinement occurs through DSR is comparable to the grain refinement through ECAP. The calculations are in accordance with these experimental results; DSR has a higher degree of non-monotonity than ESR, and the asymmetric rolling is quite near to the ECAP with respect to non-monotonity.

J.B. Lee *et al*. made investigations on the microstructure of conventional and differential speed rolled AZ31 Mg alloy sheets [25]. Theirs results show that by conventional rolling the grain refinement in the center of the sheet is less than in the upper or lower regions. This supports our assumption, the calculations for ESR show that in the center of the sheet a monotonic tension-like deformation occurs, and towards to the surface the non-monotonic shear-like deformation becomes more dominant.

6. CONCLUSION

Consider the above mentioned results and compare them to the recent calculations of non-monotonity can be established that:

(1) For processes which differ more from pure monotonic deformation (μ_1), an UFG microstructure evolves sooner.

(2) The ECAP and HPT have the highest degree of non-monotonity (μ_1), which are the most effective SPD techniques.

(3) The DNM is a qualitative value for the prognosis of grain refinement.

(4) By ECAP the value of μ_1 is equal for all routes, while the μ_2 value is sensitive to them, and changes according to the deformation routes.

The above mentioned method can be suitable for planning of production of UFG metals, enhancement of existing methods, or planning new technologies.

REFERENCES

[1] H. Saito, N. Utsunomiya and T. Tsuji // *Acta Mater* **47** (1999) 579.

[2] S.H. Lee, Y. Saito, N. Tsuji, H. Utsunomiya and T. Sakai // *Scripta Materialia* **46** (2002) 281.

[3] V. M. Segal // *Materials Science and Engineering A* **271** (1999) 322.

[4] László S. Tóth // *Computational Materials Science* **32** (2005) 568.

[5] I.V. Alexandrov, Y.T. Zhu, T.C. Lowe, R.K. Islamgaliev and R.Z. Valiev // *NanoStructured Materials.* **10** (1998) 4534.

[6] J. Y. Huang, Y. T. Zhu, H. Jiang and T. C. Lowe // *Acta Materialia* **49** (2001) 1497.

[7] G.A. Smirnov-Aljajev, *Soprotivlenie Materialov Plasticheskomu Defformirovaniju* (Mashinoctroenie, Leningrad, 1978), In Russian.

[8] V.V. Stolyarov, Y.T. Zhu, I.V. Alexandrov, T.C. Lowe and R.Z. Valiev // *Materials Science and Engineering A* **299** (2001) 59.

[9] V.G. Sinicyn and I.A. Andrujshchenko, *Teoremichnoe issledovanie protzessa nesimmetrichnoi prokatki* (Chornaja metallurgija, Moscow, 1973), In Russian.

[10] S.H. Lee and D.N. Lee // *International Journal of Mechanical Sciences* **43** (2001) 1997.

[11] M. Furukawa, Z. Horita, M. Nemoto and T.G. Langdon // *Journal of Mat. Sci.* **36** (2001) 2835.

[12] M. Kawasaki, Z. Horita and T.G. Langdon // *Materials Science and Engineering A* **524** (2009) 143.

[13] Y. Iwahashi, Z. Horita, M. Nemoto and T.G. Langdon // *Acta mater.* **45** (1997) 4733.

[14] I.V. Aleksandrov, R.G. Chembarisova, V.D. Sitdikov, G.I. Raab and V.U. Kazykhanov // *The Physics of Metals and Metallography* **104** (2007) 306.

[15] J. Gubicza, K. Máthis, Z. Hegedus, G. Ribárik and A.L. Tóth // *Journal of Alloys and Compounds* **492** (2010) 166.

[16] O. Mishin, J.R. Bowen and S. Lathabai // *Scripta Materialia* (2010).

[17] A. Mishra, B.K. Kad, F. Gregori and M.A. Meyers // *Acta Materialia* **55** (2007) 13.

[18] Y. Iwahashi, Z. Horita, M. Nemoto and T.G. Langdon // *Acta mater.* **45** (1997) 4733.

[19] V.V. Stolyarov, Y.T. Zhu, I.V. Alexandrov, T.C. Lowe and R.Z. Valiev // *Materials Science and Engineering A* **299** (2001) 59.

[20] Y. Iwahashi, Z. Horita, M. Nemoto and T.G. Langdon // *Acta mater.* **46** (1998) 3317.

[21] S.V. Dobatkin, E.N. Bastarache, G. Sakai, T. Fujita, Z. Horita and T.G. Langdon // *Materials Science and Engineering A* **408** (2005) 141.

[22] G. Sakai, Z. Horita and T.G. Langdon // *Materials Science and Engineering A* **393** (2005) 344.

[23] W.J. Kim, K.E. Lee and S.-H. Choi // *Materials Science and Engineering A* **506** (2010) 71.

[24] W.J. Kim, J.D. Park and W.Y. Kim // *Journal of Alloys and Compounds* **460** (2008) 289.

[25] J.B. Lee, T.J. Konno and H.G. Jeong // *Materials Science and Engineering B* **161** (2009) 166.